THE JOURNAL OF BIOLOGICAL CHEMISTRY VOL. 290, NO. 19, pp. 12332–12345, May 8, 2015

Estrogen-related Receptor β Reduces the Subnuclear Mobility of Estrogen Receptor α and Suppresses Estrogen-dependent Cellular Function*

Received for publication, October 17, 2014, and in revised form, March 19, 2015 Published, JBC Papers in Press, March 24, 2015, DOI 10.1074/jbc.M114.619098

Takashi Tanida[1], **Ken Ichi Matsuda, Shunji Yamada, Takashi Hashimoto, and Mitsuhiro Kawata**

From the Department of Anatomy and Neurobiology, Kyoto Prefectural University of Medicine, Kawaramachi Hirokoji, Kamigyo-ku, Kyoto 602-8566, Japan

Background: The role of orphan nuclear receptor ERRβ in estrogen-related pathophysiology is poorly understood.
Results: ERRβ repressed the transactivity of ERα and proliferation of MCF-7 breast carcinoma cells through reduction of the intranuclear mobility of ERα.
Conclusion: ERRβ affects ERα dynamics and function.
Significance: Regulation of ERRβ will provide a potential therapeutic approach for estrogen-related cancer.

Estrogen-related receptor (ERR) is a member of the nuclear receptor superfamily that has strong homology with estrogen receptor (ER) α. ERR has three subtypes (α, β, and γ) expressed in estrogen-sensitive organs, including ovary, breast, and brain. No endogenous ligands of ERRs have been identified, but these receptors share a common DNA element with ERα and control estrogen-mediated gene transcription. Recent evidence suggests a role of ERRs in estrogen-related pathophysiology, but the detailed mechanisms of ERR functions in estrogen-related tissues are unclear. Using live-cell imaging with fluorescent protein labeling, we found that only ERRβ among the ERRs exhibits a punctate intranuclear pattern overlapping with ERα following 17β-estradiol (E_2)-stimulation. Fluorescence recovery after photobleaching showed significant reduction of the mobility of ligand-activated ERα with co-expression of ERRβ. Fluorescence resonance energy transfer revealed that ERRβ directly interacts with ERα. The N-terminal domain of ERRβ was identified as the region that interacts with ERα. We also found a correlation between punctate cluster formation of ERα and interaction between the receptors. Expression of ERRβ significantly repressed ERα-mediated transactivity, whereas that of other ERR subtypes had no effect on the transactivity of ERα. Consistent with this finding, E_2-stimulated proliferation of MCF-7 breast carcinoma cells and *bcl-2* expression was significantly inhibited by expression of ERRβ. These results provide strong evidence for a suppressive effect of ERRβ on estrogen signaling through reduction of the intranuclear mobility of ERα. The findings further suggest a unique inhibitory role for ERRβ in estrogen-dependent cellular function such as cancer cell proliferation.

Estrogen receptor (ER)[2] α and β are ligand-dependent transcription factors that play critical roles in diverse pathophysiological programs, including reproduction, development, homeostasis, and cancer progression (1–3). Another subgroup in the nuclear receptor (NR) superfamily, the estrogen-related receptors (ERRs), has strong homology to ERα (4, 5). This subgroup consists of three subtypes: ERRα, ERRβ, and ERRγ. ERRs contain functional domains that are common in NRs as follows: the N-terminal domain (NTD), DNA-binding domain (DBD), hinge region, and ligand-binding domain (LBD) (6, 7). Endogenous ligands of ERRs have not been identified, and these receptors are thus referred to as orphan receptors. However, ERRs regulate the transactivity of the estrogen-response element (ERE) constitutively in an unliganded state (8, 9).

ERRα is the most abundant subtype among ERRs and is expressed at relatively high levels in organs requiring high energy, such as muscle, heart, and kidney (10–12). ERRγ is also ubiquitously expressed throughout the body and is required for spinal and cardiac tissue formation (13, 14). ERRα and -γ serve as key regulators of mitochondrial energy homeostasis through interaction with peroxisome proliferator-activated receptor γ co-activator 1-α (10, 15, 16). In contrast, expression of ERRβ is observed in restricted tissues, and disruption of the ERRβ gene causes fetal lethality resulting from impaired placentation (17, 18).

ERRs are also expressed in estrogen-responsive organs such as endometrium, ovary, and mammary gland (13, 19), and it may also be involved in estrogen-related cancers (20, 21). In breast cancer, all ERR subtypes are expressed, with proliferation stimulated by ERRα and repressed by ERRγ (22, 23). Similarly, ERRα is associated with progression and ERRγ with

* This work was supported by Grants-in-aid for Young Scientists (B) 24791116 and 26860852 (to T. T.) and for Scientific Research (B) 24300128 (to M. K.) from the Ministry of Education, Culture, Sports, Science and Technology of Japan.
[1] To whom correspondence should be addressed: Dept. of Anatomy and Neurobiology, Kyoto Prefectural University of Medicine, 465 Kajii-cho, Kawaramachi Hirokoji, Kamigyo-ku, Kyoto 602-8566, Japan. Tel.: 81-75-251-5301; Fax: 81-75-251-5306; E-mail: t-tanida@koto.kpu-m.ac.jp.

[2] The abbreviations used are: ER, estrogen receptor; AF-1, activation function-1; AF-2, activation function-2; coIP, co-immunoprecipitation; DBD, DNA-binding domain; E_2, 17β-estradiol; ERE, estrogen-response element; ERR, estrogen-related receptor; FRAP, fluorescence recovery after photobleaching; LBD, ligand-binding domain; NR, nuclear receptor; NTD, N-terminal domain; OHT, 4-hydroxytamoxifen; pAct-βgal, β-actin promoter-driven β-galactosidase expression construct; PPT, propyl pyrazole triol; CFP, cyan fluorescent protein; pen/strep, penicillin/streptomycin; ROI, region of interest; TamR, tamoxifen-resistant.

repression of ovarian cancer (24). Based on these findings, ERRα and -γ are potential diagnostic biomarkers for unfavorable and favorable prognoses, respectively, in estrogen-related cancers (25–27). A clinical study showed that ERRβ is present in normal breast adipose fibroblasts but is absent in cancer-associated fibroblasts from patients with ERα-positive breast cancer (28). These reports indicate the importance of ERRs in estrogen-related tumorigenesis, but the role and molecular mechanism of ERRβ in estrogen signaling are poorly understood.

Imaging of NRs using green fluorescent protein (GFP)-labeling has revealed a close relationship of nuclear events such as protein degradation, gene transcription, and RNA processing with subcellular dynamics (29–32). ERα localizes primarily in the nucleus, and its distribution pattern changes from diffuse to punctate in response to estrogen through attachment with nuclear meshwork components, which are referred to as the nuclear matrix (33–35).

In this study, we examined the relationship between the subcellular dynamics of ERRs in association with estrogenic stimuli and estrogen-dependent transcriptional control when co-expressed with ERα. We found a unique contribution of ERRβ to estrogen signaling, because only ERRβ among the ERRs labeled with fluorescent proteins showed punctate partitioning in the nucleus in response to 17β-estradiol (E_2) stimulation when co-expressed with ERα. The intranuclear mobility of ligand-activated ERα was reduced by direct interaction with ERRβ. Consistent with this finding, ERRβ repressed the transactivity of ERα in ERE-driven transcription and reduced proliferation of ERα-positive breast cancer cells. These findings reveal a co-regulatory pathway of estrogen signaling by classical ERα and ERRβ, and they suggest a novel hormone-response mechanism of ligand-dependent transregulation mediated by orphan NRs.

EXPERIMENTAL PROCEDURES

Plasmid Construction—Total RNA was extracted from kidney and retina of male Wistar rats using Sepasol RNA I (Nacalai Tesque, Kyoto, Japan) and reverse-transcribed with ReverTra Ace-α (Toyobo, Osaka, Japan). Synthesized cDNA encoding ERR genes was amplified by PCR with the Expand High Fidelity^{PLUS} PCR system (Roche Diagnostics). The PCR products were electrophoresed on a 1.5% agarose gel, purified using the QIAquick gel extraction kit (Qiagen, Valencia, CA), and inserted into a pGEM-T easy vector (Promega, Madison, WI). The inserts were cut with EcoRI and subcloned into a pcDNA3.1 vector (Invitrogen), a pEYFP-C1 vector (Clontech), or a pECFP-C1 vector (Clontech) at the EcoRI site. To obtain deletion mutants of pEYFP-ERRβ, the NTD, DBD, or LBD region was removed by inverse PCR using a KOD^{PLUS} mutagenesis kit (Toyobo). The deleted regions of ERRβ correspond to amino acids 1–92, 115–164, and 252–421, respectively. Inserts of each ERRβ deletion mutant were subcloned into a pEYFP-C1 vector (Clontech) at the EcoRI site. To create deletion mutants of pECFP-ERα, the insert of each deletion mutant of pEYFP-ERα was subcloned into a pECFP-C1 vector (Clontech) at the EcoRI and XhoI sites. The resulting inserts were confirmed by digestion with restriction enzymes and DNA sequencing. The details of pEC/YFP-ERα, N-terminal (dN81, dN140, and dN246) and C-terminal (dC341 and dC430) deletion mutants of pEYFP-ERα, the estrogen-response element-containing luciferase-reporter construct (ERE-Luc), and the β-actin promoter-driven β-galactosidase expression construct (pAct-βgal) have been described previously (36–38).

Cell Culture—COS-1 cells were cultured in Dulbecco's modified Eagle's medium (DMEM) (Invitrogen) supplemented with 10% fetal bovine serum (FBS) (Equitech-Bio Inc, Kerrville, TX) and 1% pen/strep solution (Invitrogen) at 37 °C in an atmosphere of 5% CO_2/air. The human breast carcinoma cell line MCF-7 (a gift from Dr. Taisuke Mori and Dr. Izumi Suganuma, Department of Obstetrics and Gynecology, Kyoto Prefectural University of Medicine) was cultured in Eagle's minimal essential medium (DS Pharma Biomedical, Osaka, Japan) supplemented with 10% FBS (Equitech-Bio), 1% nonessential amino acids solution (DS Pharma), 2 mM L-glutamine (DS Pharma), and 1% pen/strep solution (Invitrogen) under the conditions described above. Tamoxifen-resistant (TamR) cells were established from the MCF-7 cells by 3 months of continuous exposure to 10^{-6} M 4-hydroxytamoxifen (OHT) (Sigma) (39), and they were cultured in phenol red-free RPMI 1640 medium (Gibco) supplemented with 10% dextran-coated charcoal-stripped FBS (Gibco), 10^{-6} M OHT, and 1% pen/strep solution under the conditions described above. ER-negative human breast carcinoma MRK-nu-1 cells (40) (catalog no. JCRB0628; JCRB Cell Bank, Osaka, Japan) were cultured in DMEM/F-12 medium (Gibco) supplemented with 10% charcoal-dextran-stripped FBS and 1% pen/strep solution under the conditions described above.

Transfection—All plasmids were transiently transfected using Lipofectamine and Plus Reagent (Invitrogen). In live-cell imaging and transcription assays using COS-1 cells, the medium was replaced by serum-free Opti-MEM (Invitrogen) containing 1% pen/strep solution to exclude the possibility of any hormonal effects after the transfection and recovery culture. In the cell proliferation assay, the medium was replaced by phenol red-free RPMI 1640 medium supplemented with 10% dextran-coated charcoal-stripped FBS and 1% pen/strep solution after the transfection and recovery culture. For ligand stimulation, cells were treated with 10^{-7} M E_2 (Sigma) at 37 °C. The same amount of dimethyl sulfoxide (DMSO) (Nacalai Tesque) was used as control.

Time-lapse Image Acquisition—The day before transfection, 3×10^4 COS-1 cells were transferred to a 35-mm glass bottom dish (Matsunami, Osaka, Japan) pre-coated with poly-L-lysine (Sigma). The cells were transfected with 125 ng of full-length or deletion mutants of pEYFP-ERRs and/or 875 ng of full-length or deletion mutants of pECFP-ERα, as described above. Image acquisition was performed using confocal laser scanning microscopy (Carl Zeiss, Jena, Germany) using an immersion 63× objective lens. The cells were maintained in the on-stage incubation chamber at 37 °C under 5% CO_2/air. Live-cell images were acquired before and 40 min after treatment with 10^{-7} M E_2 or the same amount of vehicle (DMSO). YFP fluorescence was detected using a filter set at 514 nm excitation and 530–600 nm emission with an HFT 458/514 dichroic mirror. CFP fluorescence was observed using a filter set at 458 nm excitation and 475–525 nm emission with an HFT 458/514 dichroic

mirror. Images were analyzed using software in the confocal microscopy system (Carl Zeiss).

FRAP Analysis—Fluorescence recovery after photobleaching (FRAP) analysis was performed using confocal laser microscopy (LSM510 META). COS-1 cells seeded at 3×10^4 per 35-mm glass bottom dish pre-coated with poly-L-lysine were transfected with 125 ng of pEYFP-ERβ and/or 875 ng of pECFP-ERα, as described above. After transfection, cells were maintained in serum-free Opti-MEM for 15–24 h and then treated with 10^{-7} M E_2, ERα-specific agonist propyl pyrazole triol (PPT, 10^{-9} M) (Tocris Bioscience, Ellisville, MO), 10^{-8} M OHT, or vehicle for 1 h. Fluorescent images (25% of maximum laser power, 512 × 512 pixels, zoom factor 5, scan speed 9) of a single Z section using an immersion 63× objective lens were then taken at time intervals of 1 s after photobleaching at a wavelength of 514 nm for YFP or 458 nm for CFP at maximum laser power for 200 iterations. The time for the first scan after photobleaching was set to 0 s. A photobleach zone (ROI) in randomly selected transfected cells was defined as a circle of 50 pixels (~2.6 μm) in diameter. For quantitative analysis, fluorescence intensities of photobleached regions of 25 pixels in diameter were measured at each time point using LSM 510 software. The mean half-recovery time ($t_{½}$), the time for fluorescence to recover by 50% due to diffusion, was determined from a fluorescence recovery curve generated from 30–36 individual cells.

FRET Analysis—COS-1 cells co-transfected with pECFP-ERβ, pEYFP-ERα, pECFP-C1, or pEYFP-C1 vectors were subjected to living-cell FRET analyses (41). All FRET analyses were performed using LSM510 META confocal laser scanning microscopy and associated software (Carl Zeiss). The setup for image acquisition was as follows: 25% of maximum laser power, 512 × 512 pixels, zoom factor 6, and scan speed 6, using an immersion 63× objective lens.

The emission fingerprinting method was used to detect emission spectra. Spectral signatures were captured by λ stack acquisition with excitation at 458 nm and detection at 10-nm intervals from 456.5 to 552.8 nm using an HFT 458/543 dichroic mirror. The ROI (a circle of 20 pixels) was randomly selected from the transfected cells to obtain emission spectral patterns.

For acceptor photobleaching FRET analysis, the acceptor (YFP) of each transfected cell was photobleached using a 514-nm laser at maximum power for 250 iterations. The photobleached zone was defined as a circle of 30 pixels. Upon image acquisition, all parameters (laser power, detector gain, amplifier offset, and pinhole size) were fixed before and after photobleaching. The emission spectral patterns were obtained, and changes in donor (CFP) fluorescence intensity at 473 nm were analyzed. To visualize the changes of fluorescence intensity before and after photobleaching, the acquired images of the donor (473 nm, CFP) and acceptor (527 nm, YFP) were pseudocolored, with red and blue ranges indicating high and low intensity, respectively.

Western Blotting—COS-1 cells were transfected with pcDNA3.1-ERα, pcDNA3.1-ERRs, or full-length or deletion mutants of pECFP-ERα or pEYFP-ERRs, as described above. The following day, whole cell lysates were fractioned on 10% SDS-polyacrylamide gels and electrotransferred to Immobilon-P PVDF membranes (Millipore, Bedford, MA). ERα, ERRs, or cyan/yellow fluorescent protein-tagged receptors were detected using anti-ERα (Santa Cruz Biotechnology, Santa Cruz, CA), anti-ERRα (Epitomics, Burlingame, CA), anti-ERRβ (PPMX, Tokyo, Japan), anti-ERRγ (PPMX), or anti-GFP (Abcam, Cambridge, UK) antibodies and alkaline phosphatase-conjugated horse anti-mouse IgG (Vector Laboratories, Burlingame, CA) or goat anti-rabbit IgG antibodies (Millipore). Reactions were visualized using an nitro blue tetrazolium/5-bromo-4-chloro-3-indolyl phosphate detection kit (Nacalai Tesque).

Co-immunoprecipitation—COS-1 cells co-transfected with pcDNA3.1-ERα, pcDNA3.1-ERRs, or full-length or deletion mutants of pECFP-ERα or pEYFP-ERRs or untransfected MCF-7 cells were subjected to co-immunoprecipitation (coIP). Total cell lysates were incubated with anti-ERα, anti-ERRβ, or anti-GFP antibodies followed by incubation with protein A- or G-Sepharose beads (GE Healthcare). After incubation, lysates were washed with lysis buffer containing 1% Triton X-100, 50 mM Tris-HCl (pH 7.5), 150 mM NaCl, 1% Protease Inhibitor Cocktail (Nacalai Tesque) with and without 0.1% bovine serum albumin (Wako Pure Chemical Industries, Osaka, Japan). SDS-PAGE and Western blotting were then performed as described above.

Double Immunofluorescent Labeling—MCF-7 cells (5×10^4) were plated on 35-mm glass bottom dishes precoated with poly-L-lysine and cultured in phenol red-free RPMI 1640 medium supplemented with 10% dextran-coated charcoal-stripped FBS and 1% pen/strep solution for 24 h. Then the cells were treated with 10^{-7} M E_2 for 30 min at 37 °C and fixed with 4% paraformaldehyde in 0.1 M phosphate buffer at room temperature. After fixation, the cells were delipidated in ethanol for 30 min at −20 °C and incubated together with rabbit polyclonal antibody against ERα (Millipore) and mouse monoclonal antibody against ERRβ diluted 1:4,000 in PBS containing 1% normal goat serum (Nichirei Bioscience, Tokyo, Japan) overnight at 4 °C. Subsequently, the cells were incubated with Alexa Fluor 488-labeled anti-mouse IgG antibody (Invitrogen) and Alexa Fluor 546-labeled anti-rabbit IgG (Invitrogen) diluted 1:1,000 in PBS for 3 h at room temperature. After embedding in Vectashield (Vector Laboratories), images were collected with LSM510 META confocal laser scanning microscopy using an immersion 63× objective lens and analyzed with software provided with the microscopy system.

Transcription Assay—COS-1 cells were plated at a density of 2.5×10^4 per well on a 24-well plate (Corning Glass). The next day, cells were co-transfected with ERE-Luc (250 ng), pcDNA3.1-ERα (2.5 ng), and various amounts of pcDNA3.1-ERR (0–5 ng) vectors, as described above. pAct-βgal (100 ng) was used as internal control for the transfection efficiency. The total amount of vectors in each well was adjusted to 355 ng with pcDNA3.1 empty vector. After transfection, cells were incubated in Opti-MEM with or without 10^{-7} M E_2 for 24 h and lysed. The same amount of DMSO was used as vehicle. The luciferase and β-galactosidase activities of cell lysates were quantified using a Pica Gene luciferase assay kit (Toyo Ink, Tokyo, Japan) and a luminescent β-galactosidase detection kit II (Clontech), respectively, on the

MicroLumat^{PLUS} microplate luminometer LB96V (Berthold, Bad Wildbad, Germany).

Cell Proliferation Assay—MCF-7 (1×10^3/well), TamR (1×10^3/well), or MRK-nu-1 (3×10^3/well) cells were seeded on a 96-well plate (BD Biosciences). The next day, cells were transfected with 0–5 ng of pcDNA3.1-ERRβ vector, as described above. The total amount of expression vector in each well was adjusted to 5 ng with a pcDNA3.1 empty vector. After the transfection, MCF-7 and TamR cells were cultured in phenol red-free RPMI 1640 medium supplemented with 10% dextran-coated charcoal-stripped FBS, and 1% pen/strep solution. MRK-nu-1 cells were cultured in phenol red-free DMEM/F-12 medium supplemented with 10% dextran-coated charcoal-stripped FBS and 1% pen/strep solution after the transfection. Cell proliferation was examined with a WST-8 assay using cell counting kit-8 (CCK-8) (Dojindo Inc., Kumamoto, Japan) 3 and 5 days after transfection. In brief, 10% prewarmed CCK-8 assay solution was added to each well, and the cells were incubated for 3.5 h, after which the optical density was measured at wavelength 450 nm with a GENios microplate reader (Tecan, Männedorf, Switzerland).

Real Time RT-PCR—MCF-7 cells (5×10^4/well) were seeded on 12-well plates (Corning Glass) and transfected with 250 ng of pcDNA3.1-ERRβ or pcDNA3.1 empty vector, as described above. The next day, cells were treated with 10^{-7} M E_2 or vehicle for 2 h. Total RNA was isolated using an RNeasy micro kit (Qiagen), and 1 μg of the total RNA was reverse-transcribed, as described above. Quantitative PCR was performed using a LightCycler 480 II real time PCR instrument (Roche Diagnostics). The reaction was carried out in duplicate in 96-well plates with LightCycler® 480 Probes Master (Roche Diagnostics) and Universal Probe Library Probes (Roche Diagnostics), using the following conditions: preincubation for 10 min at 95 °C, followed by 45 cycles for 10 s at 95 °C and 25 s at 60 °C. The combinations of probes and primers were designed using online software (Probe Finder version 2.50 for human, Roche Diagnostics) as follows: *bcl-2* (probe 75), right primer 5′-AGT ACC TGA ACC GGC ACC T-3′ and left primer 5′-GCC GTA CAG TTC CAC AAA GG-3′; c-*myc* (probe 66), left primer 5′-GCT GCT TAG ACG CTG GAT TT-3′ and right primer 5′-TAA CGT TGA GGG GCA TCG-3′; *gapdh* (probe 60), left primer 5′-AGC CAC ATC GCT CAG ACA C-3′ and right primer 5′-GCC CAA TAC GAC CAA ATC C-3′. Relative gene expression levels were calculated using the comparative ΔC_p method and normalized to *gapdh* expression using software provided with the LightCycler 480 II instrument (Roche Diagnostics).

Statistical Analysis—All values were expressed as means ± S.E. Data were analyzed by unpaired *t* test or by one-way analysis of variance and Bonferroni/Dunn post hoc tests. All analyses were performed with StatView version 5.0 (SAS Institute Inc., Cary, NC). The results were considered significant if the *p* value was < 0.05.

RESULTS

Punctate Pattern of ERRβ in Response to E_2 Stimulation When Co-expressed with ERα—To examine whether ERRs respond to E_2 stimulation, time-lapse image analyses of cyan fluorescent protein-tagged ERα (CFP-ERα) and yellow fluorescent protein-tagged ERRs (YFP-ERRs) were performed after E_2 stimulation, with and without co-expression of ERRs and ERα. Protein expression of CFP-ERα and YFP-ERRs was confirmed by Western blotting from total lysates of COS-1 cells transfected with pcDNA3.1-ERα, pECFP-ERα, pcDNA3.1-ERRs (α, β, or γ), or pEYFP-ERRs (α, β, or γ). Specific antibodies against ERα, ERRα, -β, or -γ were used to detect each protein at the predicted molecular mass (Fig. 1*A*).

All the fusion proteins were mainly distributed in the nucleus (Fig. 1*B*). Diffusely distributed CFP-ERα redistributed into discrete clusters after E_2 treatment for 40 min, as shown previously (37), although none of the YFP-ERRs showed cytological changes in nuclear distribution after E_2 treatment (Fig. 1*B*). This result is consistent with the finding that ERRs do not bind to endogenous steroids (4). To examine the effect of ERα co-expression on the distribution of ERRs, co-transfection of pECFP-ERα and each pEYFP-ERR subtype was performed, and expression patterns were observed after E_2 stimulation. Interestingly, only YFP-ERRβ showed a dot-like distribution pattern that overlapped with that of CFP-ERα (Fig. 1*D*). YFP-ERRα and -γ were unchanged, and CFP-ERα showed a clear punctate expression pattern after E_2 stimulation (Fig. 1, *C* and *E*).

Endogenous ERα and ERRβ Overlap with Each Other in the Nucleus of MCF-7 Cells—Because subnuclear overlap of discrete clusters of ERα and ERRβ was observed in transfected cells, we next examined whether this phenomenon occurs for endogenous ERα and ERRβ. MCF-7 breast carcinoma cells were treated with E_2 for 30 min and stained for ERα and ERRβ by immunofluorescent labeling. Fluorescent images were acquired, and punctate patterns of overlapping endogenous ERα and ERRβ were observed (Fig. 2*A*). Using confocal laser scanning microscopy, curves approximating the fluorescence intensity along the line crossing the nuclear area were plotted (Fig. 2*B*). The intensive amplitudes for ERα and ERRβ reflect their discrete distributions. The peak fluorescence intensities of ERα (~24%) and ERRβ (~29%) also overlapped with each other, indicating co-localization of the two receptors within the punctate clusters (Fig. 2*B*, *arrowheads*). coIP analysis also confirmed a protein-protein interaction of endogenous ERα and ERRβ in MCF-7 cells treated with E_2 for 1 h (Fig. 2*C*).

ERRβ Reduces the Intranuclear Mobility of ERα Following E_2 Stimulation—Several nuclear receptors, including ERα, show ligand-dependent reduced intranuclear mobility (34, 35, 38, 42). Because YFP-ERRβ showed discrete clusters only when co-expressed with CFP-ERα, we examined whether both receptors had decreased intranuclear mobility using FRAP analyses, with a view to examine an interaction between the two receptors.

In the absence of E_2, bleach zones of CFP-ERα were not detected regardless of the presence of YFP-ERRβ because of the extreme mobility of unliganded CFP-ERα (Fig. 3, *A* and *C*), in agreement with a previous report (42). In the presence of E_2, YFP-ERRβ significantly reduced the intranuclear mobility of CFP-ERα (Fig. 3, *B* and *D–F*). The mobility of YFP-ERRβ was also decreased by ligand-activated CFP-ERα (Fig. 4, *D–F*). In the presence of the ERα-selective agonist PPT, YFP-ERRβ significantly reduced the CFP-ERα mobility (Fig. 3, *E* and *F*). Con-

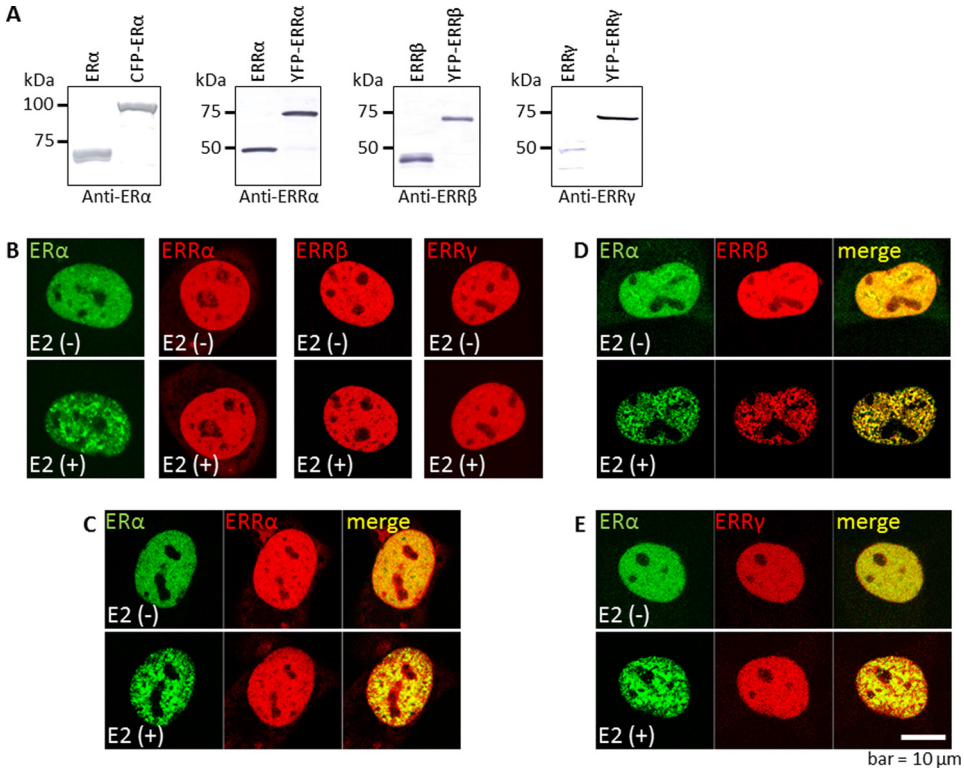

FIGURE 1. **ERRβ exhibits a punctate expression pattern in response to E_2 stimulation when co-localized with ERα.** *A*, confirmation of expression of ERα, CFP-ERα, ERRs, and YFP-ERRs. The expression plasmids pcDNA3.1-ERα, pECFP-ERα, pcDNA3.1-ERRs (α, β, or γ), or pEYFP-ERRs (α, β, or γ) were transiently transfected into COS-1 cells, and Western blotting was performed. Expression of the respective proteins was detected at the predicted molecular sizes of 67 kDa (*ERα*), 95 kDa (*CFP-ERα*), 45 kDa (*ERRα*), 67 kDa (*YFP-ERRα*), 48 kDa (*ERRβ*), 75 kDa (*YFP-ERRβ*), 51 kDa (*ERRγ*), and 78 kDa (*YFP-ERRγ*). *B–E*, time-lapse image analyses of CFP-ERα, YFP-ERRs, or combinations. COS-1 cells were transiently transfected with pECFP-ERα or pEYFP-ERRs (α, β, or γ), and time-lapse image analyses were performed before (*upper*) and 40 min after (*lower*) treatment of E2 (*B*). COS-1 cells were transiently co-transfected with pECFP-ERα and pEYFP-ERRs (α, β, or γ), and time-lapse imaging was performed before (*upper*) and 40 min after (*lower*) addition of E2. Note that YFP-ERRβ displayed a dot-like expression pattern that overlapped with CFP-ERα after E2 stimulation (*D*). *E2*, 17β-estradiol; *bar*, 10 μm.

sistent with this finding, PPT-stimulated CFP-ERα significantly reduced the mobility of YFP-ERRβ, suggesting an interaction between ERα and ERRβ (Fig. 4, *E* and *F*). This interaction appeared to be agonist-dependent because the mobility of YFP-ERRβ was not reduced in the presence of CFP-ERα under ligand-free conditions, and it was reduced only in the presence of CFP-ERα stimulated by E_2 or PPT (Fig. 4, *C–F*). Interestingly, in the presence of anti-estrogen OHT, YFP-ERRβ did not affect the mobility of CFP-ERα (Fig. 3*F*). Therefore, the mobility reduction of YFP-ERRβ seen in the presence of CFP-ERα and OHT (Fig. 4*F*) is probably due to binding of YFP-ERRβ with OHT.

A protein-protein interaction between E_2-activated ERα and ERRβ was also shown by coIP using a specific antibody against ERα or ERRβ following co-transfection of pcDNA3.1-ERα and pcDNA3.1-ERRβ expression vectors in COS-1 cells (Fig. 4*G*).

ERRβ Directly Interacts with ERα in Live Cells—We further analyzed whether ERα and ERRβ interact directly using FRET microscopy. COS-1 cells were co-transfected with pECFP-C1 and pEYFP-C1, with pECFP-ERRβ and pEYFP-C1, or with pECFP-ERRβ and pEYFP-ERα. After E_2 treatment for 1 h, images were captured using confocal laser scanning microscopy. In the emission spectral analysis, ROIs of cells co-expressing CFP-ERRβ and YFP-ERα produced FRET signals that exhibited a prominent peak at 527 nm, whereas ROIs of cells co-expressing CFP and YFP or co-expressing CFP-ERRβ and YFP did not show FRET (Fig. 5*A*).

Because FRET was clearly observed, we performed acceptor photobleaching FRET microscopy. This method is based on the increase of donor fluorescence intensity when the acceptor fluorophore is abolished in a system showing FRET. The emission spectra in Fig. 5*B* indicate that the donor intensity at 473 nm (CFP-ERRβ) was markedly increased after photobleaching of acceptor (YFP-ERα) at 514 nm. Pseudocolored images at 473 and 514 nm were acquired before and after photobleaching (Fig. 5*C*). After photobleaching, the intensity of YFP-ERα decreased (Fig. 5*C*, *lower*), whereas the intensity of CFP-ERRβ increased (Fig. 5*C*, *upper*) in the bleach zone (Fig. 5*C*, *arrowheads*). In contrast, the intensities of CFP-ERRβ and YFP-ERα in non-bleach zones did not change from before to after photobleaching (Fig. 5*C*, *arrows*). Quantification of acceptor photobleaching showed significant enhancement of fluorescence intensity (at 473 nm) of ROIs from cells co-expressing CFP-ERRβ and YFP-ERα (Fig. 5*D*). In contrast, the intensity of ROIs from cells co-expressing CFP and YFP or co-expressing CFP-ERRβ and YFP did not change after photobleaching, indicating that CFP and YFP, and ERRβ and YFP did not interact with each other and did not produce FRET (Fig. 5*D*). From these findings, we conclude that ERα and ERRβ interact directly with each other in live cells.

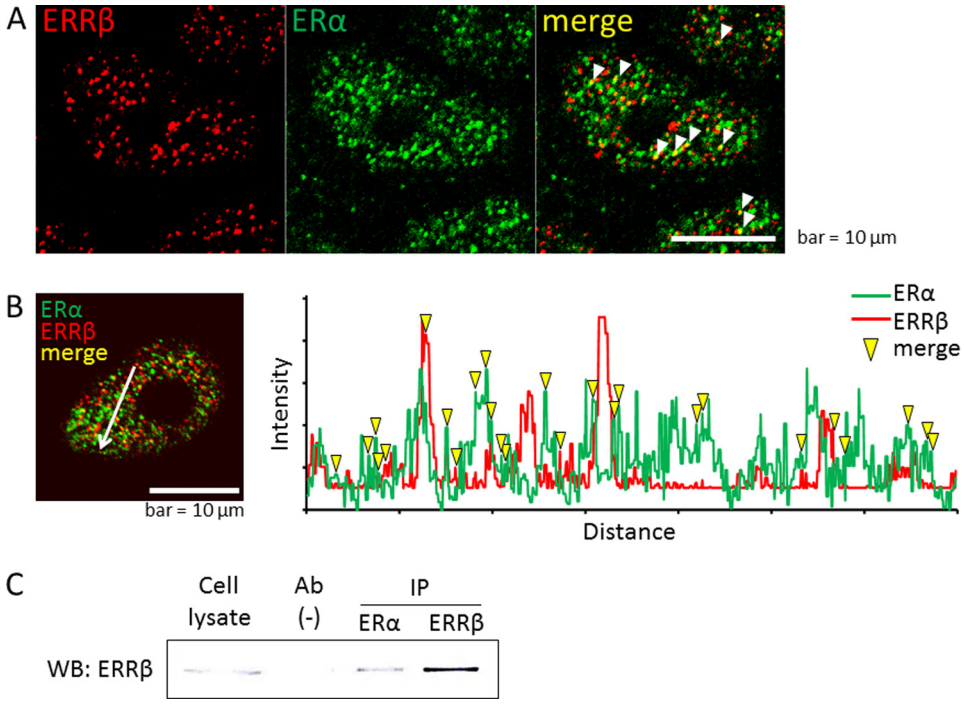

FIGURE 2. **Endogenous ERα and ERRβ exhibit discrete overlapping clusters and interact in MCF-7 cells.** *A*, MCF-7 cells were treated with E2 for 30 min and subjected to immunofluorescent staining with anti-ERα (*green*) and anti-ERRβ (*red*). *Yellow dots* represent overlap of ERα and ERRβ in the nucleus (*arrowheads*). All images were captured using confocal laser scanning microscopy. *B*, fluorescence intensities of ERα and ERRβ along the *white arrow* in the *left panel* are plotted with *green* (ERα) and *red* (ERRβ) curves, respectively. *Yellow arrowheads* are the positions where the fluorescence peaks of ERα and ERRβ overlap. *C*, protein-protein interaction between endogenous ERα and ERRβ. MCF-7 cells were treated with E2 for 1 h, and total cell lysates were subjected to coIP. Lysates without immunoprecipitation (*Cell lysate*) and lysates immunoprecipitated without antibody (*Ab*(-)) were loaded as controls. *coIP*, co-immunoprecipitation; *E2*, 17β-estradiol; *WB*, Western blot; *Ab*, antibody; *bar*, 10 μm.

ERRβ Contributes to Cluster Formation of ERα—Using the deletion mutants of YFP-ERα shown in Fig. 6*A*, Matsuda *et al.* (37) demonstrated that the ligand-induced clustering activity of ERα depends on the latter part of AF-1 within the NTD, the DBD, or AF-2 within the LBD. COS-1 cells were co-transfected with the deletion mutants of pECFP-ERα and full-length pEYFP-ERRβ, and live-cell imaging was performed. Protein expression of the deletion mutants was confirmed by Western blotting from total lysates of COS-1 cells transfected with each expression plasmid (Fig. 6, *B* and *C*).

When co-expressed with ERRβ, dN81 and dN140 exhibited dot-like expression patterns following E_2 stimulation, whereas dN246, dC341, and dC430 did not do so (Fig. 6, *E–I*). dN140 itself does not have clustering activity in response to E_2 (Fig. 6*A*). Therefore, these results show that ERRβ can recover the clustering activity of the latter part of AF-1 of ERα. Similarly, coIP showed that dN81 and dN140 interact with ERRβ, whereas dN246, dC341, and dC430 did not show this interaction, suggesting that cluster formation overlapping with each other is critical for the interaction between the two receptors (Fig. 6*J*). Because dN246, dC341, and dC430 lack the activity to bind with DNA or ligand, or to dimerize, these activities may be required for the interaction with ERRβ.

ERRβ Interacts with ERα through the N-terminal Domain—To identify which domain of ERRβ is required for interaction with ERα, deletion mutants of ERRβ tagged with YFP were generated. The schematic structures of these deletion mutants are shown in Fig. 7*A*. Protein expression of the mutants was confirmed by Western blotting from total lysates of COS-1 cells transfected with each expression plasmid (Fig. 7*B*).

pECFP-ERα and expression plasmids of the deletion mutants were co-transfected into COS-1 cells, and live-cell imaging was performed. After E_2 stimulation, dNTD did not form discrete clusters that overlapped with CFP-ERα, although other deletion mutants of dDBD and dLBD exhibited dot-like expression patterns that overlapped with CFP-ERα (Fig. 7, *C–F*). In coIP, binding with ERα was undetected for dNTD, whereas dDBD and dLBD bound to ERα (Fig. 7*G*). These results show that the NTD of ERRβ interacts with clustered ERα.

ERRβ Represses the Transcriptional Activity of ERα—Because the intranuclear mobility of ERα was decreased by direct interaction with ERRβ (Figs. 3 and 5), we examined whether the transcriptional activity of ERα was affected by ERRβ using an ERE-driven luciferase reporter assay. COS-1 cells were co-transfected with pcDNA3.1-ERα and various amounts of pcDNA3.1-ERRβ and were incubated in the presence or absence of E_2 for 20 h. Then normalized luciferase activity was determined. As shown in Fig. 8, *A–C*, ERRβ reduced the ERα-mediated transcriptional activity of ERE in a dose-dependent manner, whereas ERRα and -γ appeared to have no effect on the transactivity of ERα. These results suggest that the punctate expression pattern of ERRβ and the correlated reduced mobility of ERα are associated with transcriptional suppression (Figs. 1–3).

ERRβ Inhibits Estrogen-dependent Cellular Proliferation of MCF-7 Breast Cancer Cells—We further speculated that ERRβ has the potential to reduce estrogen-dependent cellular func-

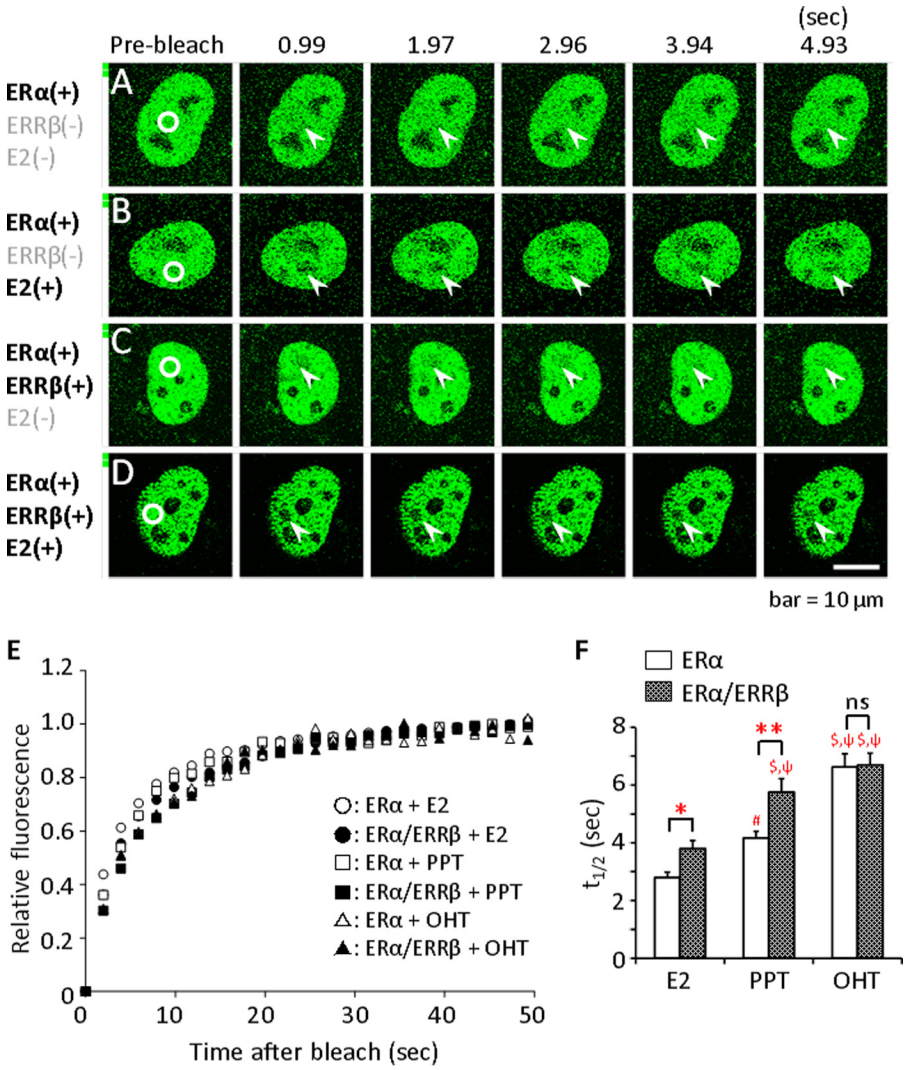

FIGURE 3. **ERRβ reduces the intranuclear mobility of ERα stimulated by agonist.** *A–D,* single transfection of pECFP-ERα (*A* and *B*) or co-transfection with pECFP-ERα and pEYFP-ERRβ (*C* and *D*) was carried out in COS-1 cells. After incubation for 15 h, cells were treated with E_2 (*B* and *D*) or the same amount of vehicle (*A* and *C*) for 1 h, after which FRAP analyses of CFP were performed. *Circles* and *arrowheads* indicate bleached zones. *E*, CFP recovery curves of FRAP for cells expressing CFP-ERα treated with E_2 (*open circles*), co-expressing CFP-ERα and YFP-ERRβ treated with E_2 (*filled circles*), expressing CFP-ERα treated with PPT (*open squares*), co-expressing CFP-ERα and YFP-ERRβ treated with PPT (*filled squares*), expressing CFP-ERα treated with OHT (*open triangles*), and co-expressing CFP-ERα and YFP-ERRβ treated with OHT (*filled triangles*). The time of initial fluorescence intensity after bleaching was set to 0 s, and plateau values were set as 1.0. *F*, quantification of FRAP analyses. Note that ERRβ significantly reduced the mobility of ERα stimulated by E_2 or PPT. Data are shown as mean ± S.E. (n = 32–35). *, $p < 0.05$; **, $p < 0.01$; #, $p < 0.01$ *versus* CFP-ERα with E_2; $, $p < 0.001$ *versus* CFP-ERα with E_2; ψ, $p < 0.001$ *versus* CFP-ERα and YFP-ERRβ with E_2; *ns*, not significantly different (*F*). *E2*, 17β-estradiol; *FRAP*, fluorescence recovery after photobleaching; $t_{1/2}$, half-recovery time; *OHT*, 4-hydroxytamoxifen; *PPT*, propylpyrazole triol; *bar,* 10 μm.

tion. To examine this issue, the effect of ERRβ on proliferation of MCF-7 cells, an estrogen-sensitive breast carcinoma cell line, was analyzed. Expression of ERα was confirmed by Western blotting from a total lysate of MCF-7 cells. The total cell lysate of COS-1 cells transfected with pcDNA3.1-ERα was used as a positive control (Fig. 9*A*).

MCF-7 cells transfected with pcDNA3.1-ERRβ were incubated with or without E_2. Cell proliferation was determined using a WST-8 assay at 3 and 5 days after transfection. Proliferation of MCF-7 cells stimulated with E_2 was significantly reduced by expression of ERRβ at 3 and 5 days after transfection (Fig. 9*B*). ERRβ had no effect on proliferation in E_2-untreated groups (Fig. 9*B*). These results show that ERRβ-mediated reduction of ERα mobility results in inhibition of estrogen-dependent cellular function. To examine the effect of ERRβ on estrogen-insensitive activity, TamR cells, which exhibit estrogen-independent proliferation, were established from MCF-7 cells (data not shown) (39, 43). Expression of ERRβ did not affect the estrogen-independent proliferation of TamR cells at 3 and 5 days after transfection (Fig. 9*C*), suggesting that suppression of estrogen signaling by interaction of ERα and ERRβ is ineffective in estrogen-irresponsive cells.

ERRβ Selectively Suppresses Estrogen-dependent Gene Expression—Several genes, including *bcl-2* and c-*myc*, are regulated in an estrogen-dependent manner in breast cancer cells (44) and exert anti-apoptotic and oncogenic effects, respectively. Because a growth inhibitory effect of ERRβ was observed in E_2-stimulated MCF-7 cells (Fig. 9*B*), we examined whether estrogen-dependent gene expression is affected by expression of ERRβ. After treatment with E_2 or vehicle for 2 h, mRNA

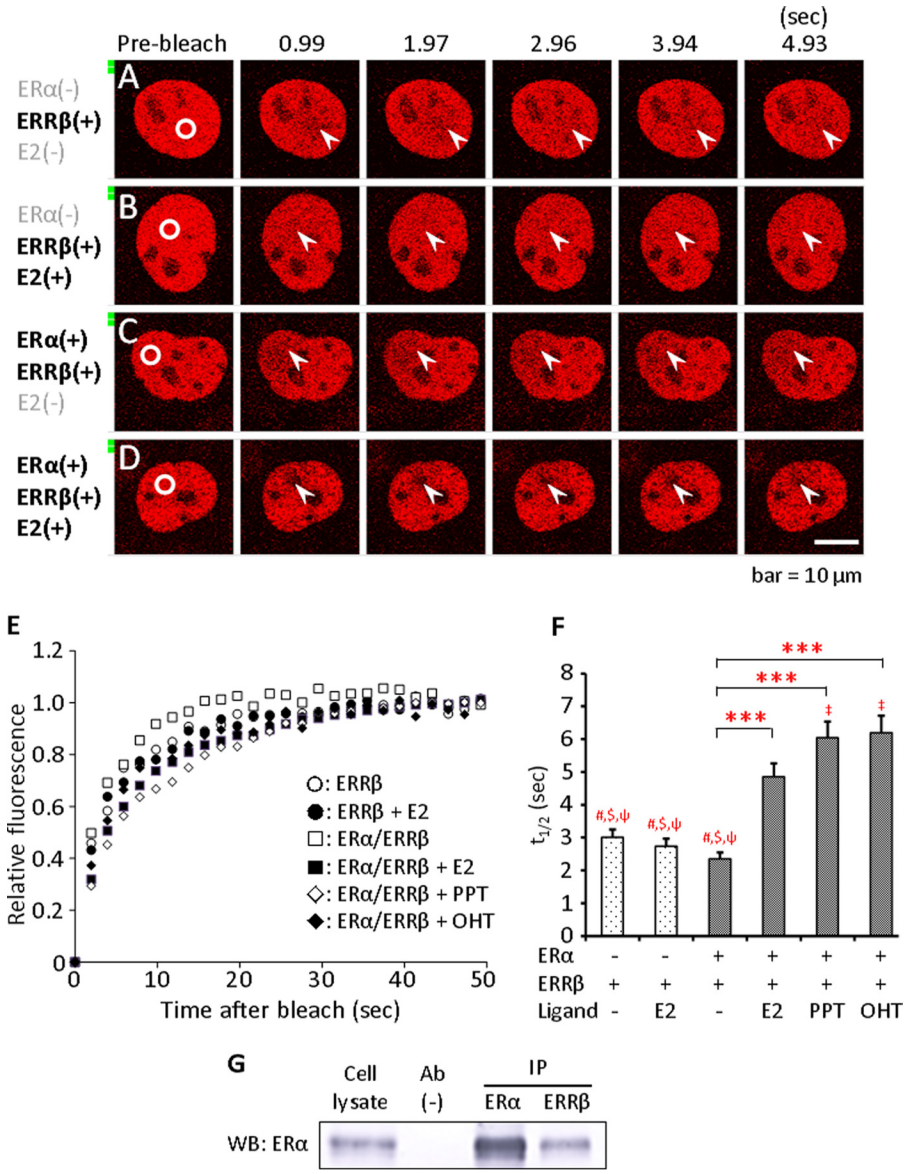

FIGURE 4. **Intranuclear mobility of ERRβ is reduced by ligand-activated ERα by interaction between the two receptors.** *A–D*, single transfection of pEYFP-ERRβ (*A* and *B*) or co-transfection with pECFP-ERα and pEYFP-ERRβ (*C* and *D*) was carried out in COS-1 cells. After incubation for 15 h, the cells were treated with E_2 (*B* and *D*) or the same amount of vehicle (*A* and *C*) for 1 h, after which FRAP analyses on YFP were performed. *Arrowheads* and *circles* indicate bleached zones. *E*, FRAP YFP recovery curves for cells expressing YFP-ERRβ without E_2 (*open circles*) and with E_2 (*filled circles*); co-expressing CFP-ERα and YFP-ERRβ without E_2 (*open squares*) and with E_2 (*filled squares*); and co-expressing CFP-ERα and YFP-ERRβ with PPT (*open diamonds*) and OHT (*filled diamonds*). The time of initial fluorescence intensity after bleaching was set to 0 s, and plateau values were set to 1.0. *F*, quantification of FRAP data. Note that in the presence of ERα, ERRβ mobility was reduced in treatment with E_2, PPT, or OHT. Data are shown as mean ± S.E. ($n = 30–36$). ***, $p < 0.001$. #, $p < 0.001$ *versus* CFP-ERα and YFP-ERRβ with E_2; $, $p < 0.001$ *versus* CFP-ERα and YFP-ERRβ with PPT; ψ, $p < 0.001$ *versus* CFP-ERα and YFP-ERRβ with OHT; ‡, $p < 0.05$ *versus* CFP-ERα and YFP-ERRβ with E_2. *G*, protein-protein interaction between ERα and ERRβ. COS-1 cells were transiently co-transfected with pcDNA3.1-ERα and pcDNA3.1-ERRβ. After incubation for 15 h and E_2 treatment for 1 h, total cell lysates were subjected to coIP. *E2*, 17β-estradiol; FRAP, fluorescence recovery after photobleaching; $t_{1/2}$, half-recovery time; *Ab*, antibody; *coIP*, co-immunoprecipitation; *OHT*, 4-hydroxytamoxifen; *PPT*, propylpyrazole triol; *WB*, Western blot; *bar*, 10 μm.

expression for *bcl-2* and c-*myc* in MCF-7 cells transiently transfected with pcDNA3.1-ERRβ or pcDNA3.1 empty vector was analyzed by real time RT-PCR. The E_2-activated expression of *bcl-2* mRNA was significantly repressed by ERRβ (Fig. 9*D*), whereas the expression level of c-*myc* mRNA was not affected by expression of ERRβ in E_2-treated and untreated cells (Fig. 9*E*).

DISCUSSION

Ligand-activated ERα recruits other cofactors to organize transcription machinery associated with the nuclear matrix (33, 34, 45). ERα is extremely mobile in a ligand-free condition, whereas the mobility is reduced following ligand binding due to attachment to the nuclear matrix (35, 46). This step is crucial for ligand-dependent biological processes common among steroid hormone receptors (47).

The present FRAP and coIP analyses demonstrated that interaction with ERRβ further slows the mobility of agonist-stimulated ERα, and the transcription assay revealed ERRβ-induced transcriptional repression of ERα in the presence of E_2. Transcriptional repression of ERα concomitant with further mobility reduction is also observed in the co-expression of scaf-

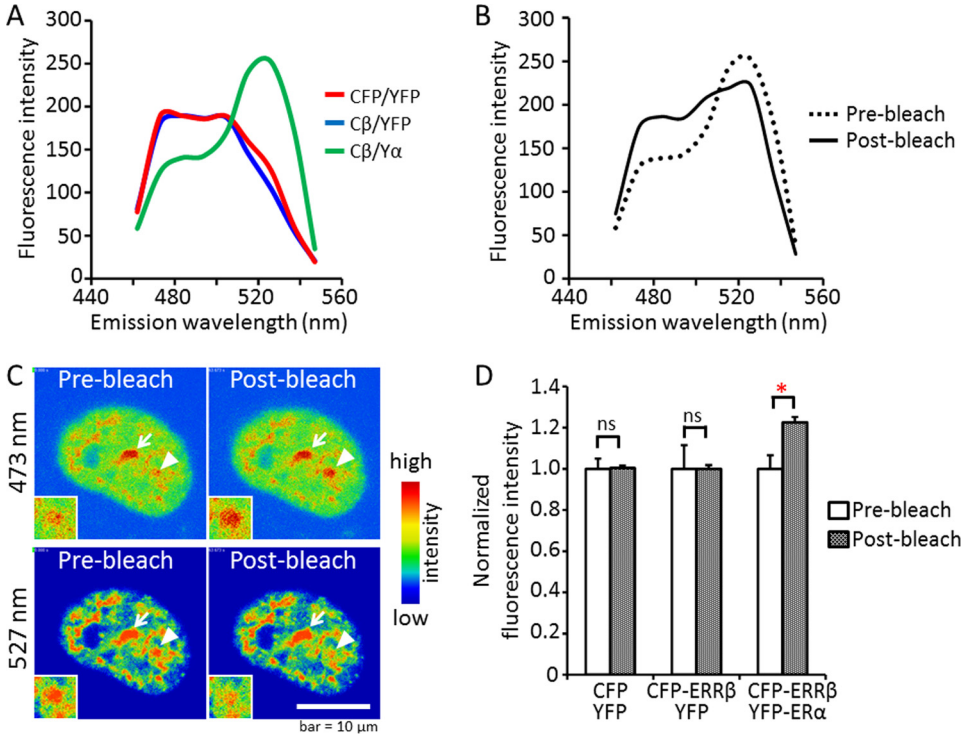

FIGURE 5. **FRET revealed a direct interaction between ERα and ERβ in live cells.** *A*, emission-spectral analysis of FRET images in live cells. Spectral curves from ROIs in COS-1 cells co-expressing CFP and YFP (*red*), CFP-ERRβ and YFP (*blue*), or CFP-ERRβ and YFP-ERα (*green*) treated with E2 for 1 h are shown. Note that the spectrum from cells co-expressing CFP-ERRβ and YFP-ERα exhibits a strong peak at 527 nm. *B–D,* acceptor photobleaching analysis of live-cell FRET imaging. *B*, emission spectra from pre- (*dotted curve*) and post- (*solid curve*) bleached ROIs of COS-1 cells co-expressing CFP-ERRβ and YFP-ERα. The ROI was photobleached at 514 nm, and immediately the peak at 527 nm decreased, whereas the peak at 473 nm increased. *C*, pseudocolor images of pre- (*left*) and post- (*right*) bleaching. Images of cells co-expressing CFP-ERRβ and YFP-ERα were captured at 473 nm (for CFP-ERRβ, *upper*) and 527 nm (for YFP-ERα, *lower*). *Arrowheads* and *arrows* indicate bleached and nonbleached regions, respectively. Magnified images of pre- and post-bleached region (*arrowheads*) are also included. Note that the CFP-ERRβ signal is enhanced (*upper right*, *arrowheads*), although the YFP-ERα signal is decreased (*lower right*, *arrowheads*) after photobleaching. *bar,* 10 μm. *D,* comparison of donor (at 473 nm) fluorescence intensity between pre- and post-bleached ROIs. COS-1 cells co-expressing CFP and YFP, CFP-ERRβ and YFP, or CFP-ERRβ and YFP-ERα were subjected to acceptor photobleaching. The fluorescence intensity was normalized to the pre-bleach level in each group. Data are shown as mean ± S.E. (n = 12–16). *, $p < 0.05$; *ns*, not significantly different; *Cβ*, CFP-ERRβ; *Yα*, YFP-ERα; *FRET,* fluorescence resonance energy transfer.

fold attachment factor B1/2, which mediates binding with the nuclear matrix (38). This report and our present findings support the idea that attachment of ERα with protein components results in transcriptional repression. However, the molecular mechanism underlying the correlation between transactivity and nuclear mobility of ERα is unclear. Alteration of subnuclear mobility of ERα affects its contact frequency with response elements and may reflect exchange of transcriptional co-regulators (48–52). Therefore, the mechanism of action of ERRβ may involve prevention of access of ERα to the ERE or, alternatively, co-regulator exchange from co-activators to co-repressors by binding with ERRβ. Further studies are required to identify how ERRβ represses the transactivity of ERα by reducing its intranuclear mobility.

Interestingly, in the presence of the anti-estrogen OHT, the mobility of ERα was not affected by co-expression with ERRβ, whereas OHT significantly reduced the mobility of ERRβ when co-expressed with ERα. These results suggest that, in contrast to E_2 or PPT, OHT-bound ERα did not interact with ERRβ, and ERRβ mobility was reduced by binding with OHT independent of ERα. These data support the idea that recruited cofactors of ERα differ if the bound ligand is an agonist or antagonist (53, 54).

The discrete cluster formation activity of ERα depends on binding with the nuclear matrix (46). The dN81 ERα mutant retains clustering activity, but others, including dN140, dN246, dC341, and dC430, do not show this activity (37). These results confirmed that dN81 and dN140 possess the ability to form discrete clusters overlapping with ERRβ, whereas dN246, dC341, and dC430 do not have this ability (Fig. 4). Therefore, the redistribution activity of ERα associated with ERRβ overlapping is retained within amino acids 140–246, which include the latter part of AF-1, or amino acids 341–600, which include LBD and AF-2. Interestingly, co-localization with intact ERα (37) or even ERRβ (Fig. 4*F*) recovered the clustering activity of dN140 following E2 stimulation. These findings suggest that the presence of AF-1 of ERα or ERRβ is sufficient to form a discrete cluster, although AF-1 in the two receptors has little similarity (55). This also indicates that ERRβ is not just passively recruited by ERα but helps with the clustering activity of ERα, despite ERRβ not responding to E2 (7). As expected, ERα deletion mutants lacking AF-2, including dC341 and dC430, did not form clusters in the presence or absence of ERRβ, because they fail to bind with E_2.

ERα and -β activate transcription following ligand binding as homodimers and a heterodimer (56). Dimerization is mediated by the dimer interface within the LBD (57). In contrast, ERRs stimulate transcription of ERE-containing genes as both monomers and homo/heterodimers (58–60). Because the dimer interface of ERRβ is located within the LBD, we first examined

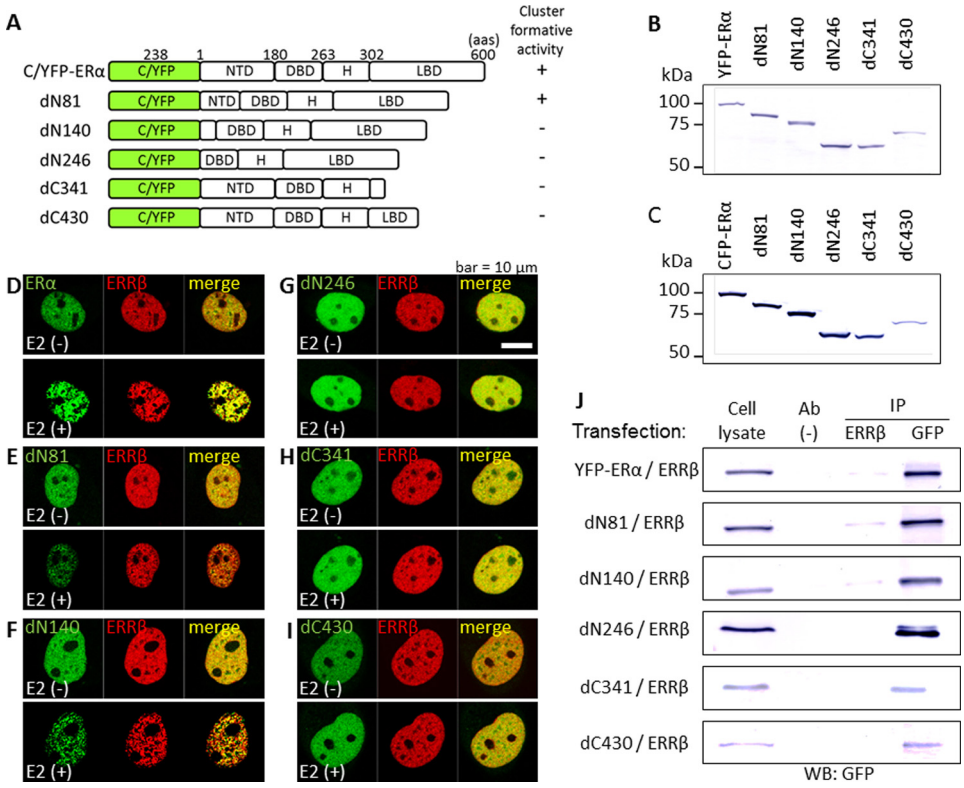

FIGURE 6. **Protein regions of ERα required for interaction with ERRβ.** *A*, schematic model and discrete cluster formation activity of C/YFP-ERα and deletion mutants. *B* and *C*, characterization of C/YFP-ERα and deletion mutants. COS-1 cells were transiently transfected with expression plasmids of pEC/YFP-ERα and deletion mutants, and total cell lysates were subjected to Western blotting (*WB*) using specific antibodies against GFP. Expression of these proteins was detected at the predicted molecular sizes of 95 kDa (*C/YFP-ERα*), 85.4 kDa (*dN81*), 79.1 kDa (*dN140*), 67.1 kDa (*dN246*), 64.5 kDa (*dC341*), and 74.6 kDa (*dC430*). *D–I*, time-lapse imaging of full-length or deletion mutants of CFP-ERα and YFP-ERRβ co-expressed in COS-1 cells. After incubation for 15 h, time lapse-image analyses were performed before (*upper*) and after (*lower*) treatment with E_2 for 40 min. *J*, coIP analyses of YFP-ERα, its deletion mutants, and ERRβ. COS-1 cells were co-transfected with full-length or deletion mutants of YFP-ERα and pcDNA3.1-ERRβ. After incubation for 15 h following E_2 treatment for 1 h, total cell lysates were immunoprecipitated (*IP*) with the indicated antibodies and blotted with anti-GFP antibody. Lysates without immunoprecipitation (*Cell lysate*) and lysates immunoprecipitated without antibody (*Ab*(−)) were loaded as controls. *H,* hinge region; *E2*, 17β-estradiol; *bar,* 10 μm.

whether the binding domain of ERRβ with ERα is located in the LBD. However, contrary to our expectation, the potential binding site was determined to be within the NTD by live-cell imaging and coIP using deletion mutants of ERRβ. In contrast, the interaction has been predicted to depend on the D-domain and LBD by computer modeling (61). The reason for the different findings may be the contrast between computer-assisted three-dimensional modeling and live cell-imaging/coIP using deletion mutants of ERRβ. *In vivo* experiments are affected by many conditions, such as cell context, cofactors of receptors, and other intracellular components, in comparison with an *in silico* study. FRET microscopy, including emission-spectral analysis and acceptor photobleaching, showed a direct interaction between ERα and ERRβ in live cells. Therefore, we suggest that the NTD of ERRβ provides a direct binding interface for ERα.

The NTD of NRs, including ERRs, possesses an AF-1 region that is unfolded and functions independently of ligand stimulation. Several reports suggest that this unfolded AF-1 structure is essential for recruitment of transcriptional co-regulators (62, 63). Thus, we propose a model in which AF-1 within the NTD of ERRβ recognizes ligand-activated ERα as a transcriptional cofactor, and their interaction causes transcriptional repression of ERα. Many transcriptional co-regulators such as SRC-1 and RIP140 possess the L*XX*LL motif for interaction with NRs, including ERα (64). ERRβ contains this signature motif within the LBD, rather than the NTD. However, the NTD of ERRβ has at least four signature (I/L)*XX*(L/H/I) motifs at positions 27–30, 30–33, 49–52, and 95–98 (NCBI Protein Database under NCBI accession number NP_001008516.2) that are responsible for co-repressor protein interactions with NRs, including ERα (53, 65). This sequence is referred to as a co-repressor-nuclear receptor box and may function as a binding surface of ERα that causes transrepression, as confirmed for co-repressors. ERα and ERβ have been suggested to bind as a heterodimer in response to estrogen (37, 57, 66). ERRβ can also form a heterodimer with ERRα that leads to transactivation of ERE and can interact with ERβ, with the resulting modulation of breast cancer-related genes (61, 67). Given that the dimer interface of ERRβ is located within its LBD, while ERRβ interacts with ERα through the NTD, a more complicated complex (trimer or tetramer) of ERs and ERRs centered on ERRβ may be possible, suggesting multiple signaling pathways of estrogen action.

ERRβ includes three splicing variants as follows: hERRβ2, hERRβ2-Δ10, and short-form hERRβ (55). Short-form hERRβ is a widely expressed human homolog of mouse and rat ERRβ, whereas expression of hERRβ2 and hERRβ2-Δ10 is restricted to testis and kidney (55). Short-form ERRβ cloned from rat tissue was used in this study, which makes it highly probable that our findings can be extrapolated to human pathophysiol-

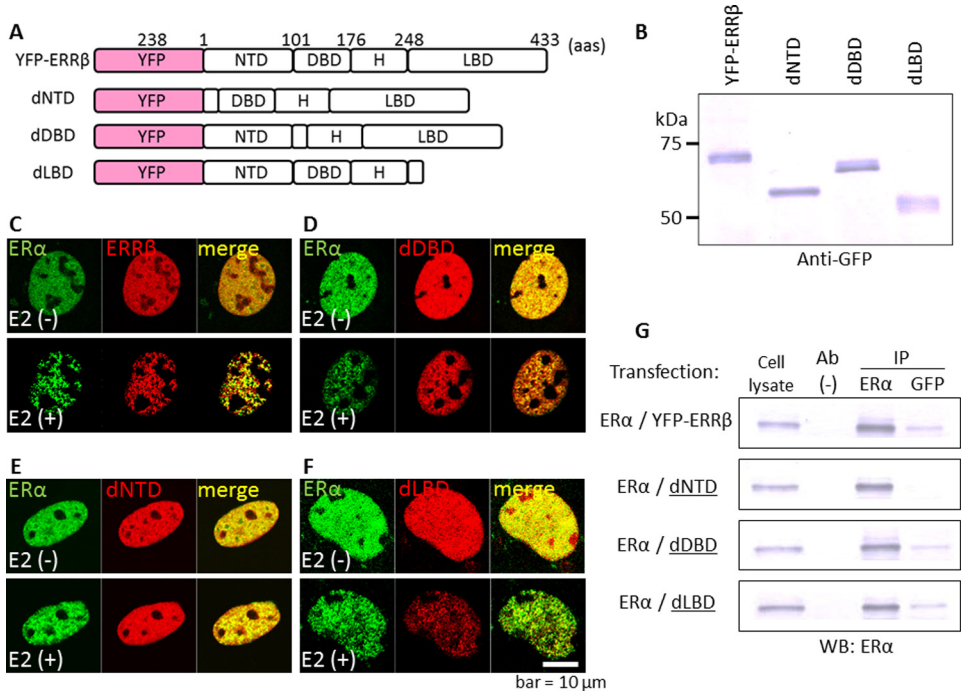

FIGURE 7. **ERRβ requires its N-terminal domain for interaction with ERα.** *A*, schematic domain structures of YFP-ERRβ and deletion mutants. *B*, characterization of YFP-ERRβ and deletion mutants. COS-1 cells were transiently transfected with expression plasmids of pEYFP-ERRβ and deletion mutants, and total cell lysates were subjected to Western blotting (*WB*) using specific antibodies against GFP. The fusion proteins displayed the predicted molecular masses of 75.3 kDa (*YFP-ERRβ*), 66 kDa (*dNTD*), 69.5 kDa (*dDBD*), and 55.4 kDa (*dLBD*). *C--F*, time-lapse image analyses of CFP-ERα, YFP-ERRβ, and deletion mutants. COS-1 cells were transiently co-transfected with pECFP-ERα and pEYFP-ERRβ or deletion mutants. After incubation for 15 h, live-cell imaging was performed before (*upper*) and after (*lower*) E_2 treatment for 40 min. Note that dNTD did not show any changes, whereas dDBD and dLBD exhibited dot-like expression patterns that overlapped with CFP-ERα after E_2 stimulation. *G*, coIP analyses of CFP-ERα, YFP-ERRβ, and deletion mutants. COS-1 cells were transiently co-transfected with pcDNA3.1-ERα and pEYFP-ERRβ or deletion mutants. After incubation for 15 h following E_2 treatment for 1 h, total cell lysates were immunoprecipitated (*IP*) with the indicated antibodies and blotted by anti-ERα antibody. Lysates without immunoprecipitation (*Cell lysate*) and lysates immunoprecipitated without antibody (*Ab*(−)) were loaded as controls. *H*, hinge region; *E2*, 17β-estradiol; *DBD*, DNA-binding domain; *LBD*, ligand-binding domain; *NTD*, N-terminal domain; *bar*, 10 μm.

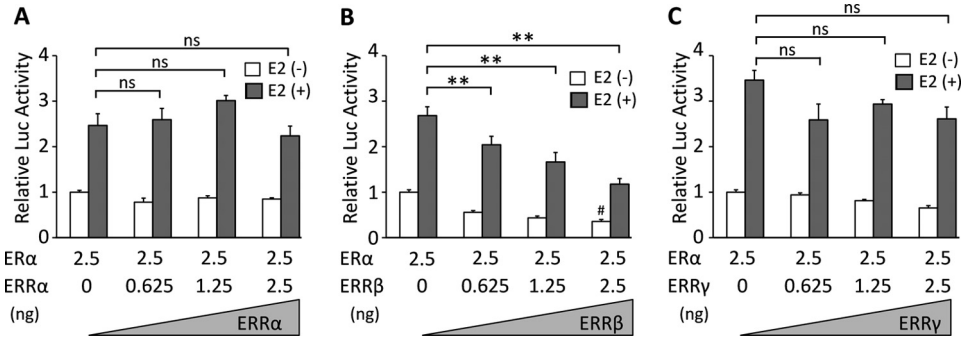

FIGURE 8. **ERRβ represses the ERα-mediated transcriptional activity of ERE.** COS-1 cells were co-transfected with ERE-Luc (250 ng), pAct-βgal (100 ng), pcDNA3.1-ERα (2.5 ng), and pcDNA3.1-ERRα (*A*), β (*B*), or γ (*C*) (0–2.5 ng). The total amount of expression vector in each well was adjusted to 5 ng with pcDNA3.1 empty vector. The cells were incubated with E_2 (*shaded bars*) or without E_2 (*white bars*) for 24 h, and luciferase activity was determined by normalization using a β-galactosidase activity. Note that ERRβ significantly repressed the transcriptional activity of ERα-mediated transactivity of ERE in a dose-dependent manner. Data are shown as mean ± S.E. ($n = 6$). *ns*, not significantly different; **, $p < 0.01$; #, $p < 0.01$ *versus* $E_2(-)$ control; *ERE-Luc*, estrogen-response element-driven luciferase reporter; *pAct-βgal*, β-actin promoter driven β-galactosidase expression construct; *E2*, 17β-estradiol.

ogy. Indeed, short-form ERRβ reduces proliferation of Ishikawa cells, an ERα positive-endometrial adenocarcinoma cell line (68), supporting our functional studies on ERRβ, as discussed below.

ERRβ-specific transcriptional repression of ERE-driven luciferase activity mediated by ERα further prompted us to analyze the estrogen-dependent cellular functions of ERRβ. Our data indicated that ectopic expression of ERRβ significantly reduced E_2-activated proliferation of estrogen-sensitive MCF-7 cells. In contrast, estrogen-independent proliferation of TamR cells was not affected by expression of ERRβ. In addition, E_2-activated *bcl-2* expression was repressed by expression of ERRβ in MCF-7 cells. Taken together, cellular processes mediated through endogenous ERα can be inhibited by ERRβ following estrogenic stimulation, and ERRβ is functionally integrated into estrogen signaling that controls cellular properties. Because BCL-2 protein has an anti-apoptotic function (44), at least one of the tumor-suppressive effects of ERRβ occurs through a pro-apoptotic action. However, E_2-stimulated c-*myc* expression was not affected by expression of ERRβ. Therefore,

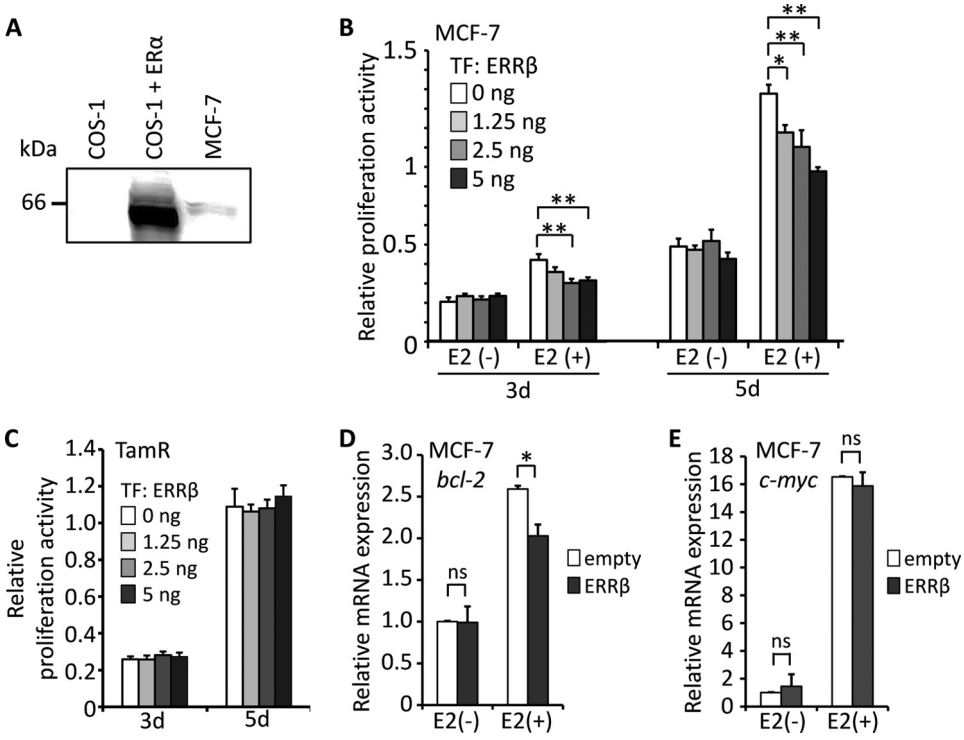

FIGURE 9. **ERRβ inhibits estrogen-dependent function of MCF-7 cells.** *A*, total lysates of naive COS-1 cells (*left*), COS-1 cells transiently transfected with pcDNA3.1-ERα (*middle*), or MCF-7 breast carcinoma cells (*right*) were subjected to Western blotting using a specific antibody against ERα. *B*, MCF-7 cells were transfected with 0–5 ng of pcDNA3.1-ERβ as indicated. The total amount of expression vector was adjusted to 5 ng with pcDNA3.1 empty vector. The cells were incubated with E_2 (*right*) or without E_2 (*left*) for 3 and 5 days after transfection. Cell proliferation activity was then examined with a WST-8 assay using CCK-8 by analyzing the optical density at wavelength of 450 nm. Data are shown as mean ± S.E. ($n = 4$). *C*, TamR cells were transfected with 0–5 ng of pcDNA3.1-ERβ, as described above, and incubated in the presence of OHT for 3 and 5 days. Cell proliferation was then examined as described above. Note that expression of ERβ did not affect proliferation of TamR cells. Data are shown as mean ± S.E. ($n = 6$). *D* and *E*, ERβ selectively suppresses estrogen-dependent gene expression. MCF-7 cells were transiently transfected with pcDNA3.1-ERβ (250 ng) or the same amount of pcDNA3.1 empty vector and treated with E_2 or vehicle for 2 h. Total RNA from the cells was subjected to real time RT-PCR for quantification of the mRNA expression levels of *bcl-2* (*D*) and c-*myc* (*E*). Each value was normalized to the *gapdh* expression level and is shown as fold activation relative to the value of a vehicle-treated group transfected with an empty vector. Data are shown as mean ± S.E. ($n = 6$). *, $p < 0.05$; **, $p < 0.01$; *ns*, not significantly different; *E2*, 17β-estradiol; *OHT*, 4-hydroxytamoxifen; *TamR*, tamoxifen resistant.

some target genes of ERα are affected, and some are unaffected by ERβ following estrogenic stimulation.

Several studies, including clinical findings, suggest an inverse association between the ERβ expression level and estrogen-dependent tumor progression (25, 26, 28). Our findings support this idea, but a variety of mechanisms has been proposed in other reports. A recent report suggests that ERβ expression results in a better prognosis in breast cancer patients with reduced *BCA2* and an increased *FST* level by controlling these genes (61). In addition, ERβ exerts a carcinostatic effect through activation of the *p21* tumor suppressor gene and cell cycle regulation, which are not linked to anti-estrogenic action (69, 70). In fact, our proliferation assay in MRK-nu-1 triple-negative breast cancer cells indicated a growth inhibitory action of ERβ independent of estrogen signaling (data not shown). In contrast, as described above, the basal growth activity of E_2-untreated MCF-7 cells or E_2-independent proliferation of TamR cells was not affected by expression of ERβ. Thus, the carcinostatic effect of ERβ through an estrogen-independent pathway is cell line- or condition-specific.

Overall, our findings provide new understanding of ERβ effects on estrogenic action in association with intranuclear mobility of ERα. The results also show the pathological and therapeutic importance of ERβ in estrogen-dependent oncodevelopment and tumorigenesis. Hormone-dependent gene transcription is regulated by a complex network of interactions with other proteins in the transcriptional machinery. An orphan NR such as ERβ may be a potential regulator behind this exquisite control of gene transcription, underlying modulation of sensitivity to hormones and selection of target genes within each organ or cell. Thus, we propose a model of a hormone response mechanism based on subnuclear trafficking, *i.e.* orphan NR-mediated transregulation initiated by steroid hormones.

Acknowledgments—We are grateful to Drs. Taisuke Mori, Izumi Sugananuma, and Seiki Matsuo (Department of Obstetrics and Gynecology, Kyoto Prefectural University of Medicine) for their kind gift of MCF-7 breast carcinoma cells. Professor Mayumi Nishi (Department of Anatomy and Cell Biology, Nara Medical University) and Dr. Takashi Ueda (Department of Urology, Kyoto Prefectural University of Medicine) gave us insightful suggestions. Colleagues in our laboratory, including Dr. Keiko Takanami, Dr. Natsuko Kaku, Taisuke Uemura, Yuki Takeda, Emiri Takemaru, Yu Sakaue, Atsuki Ohta, Amane Matsu-ura, Miku Ohya, Mari Tsuboi, and Kayo Tanida, are acknowledged for helpful discussions and technical support.

REFERENCES

1. Kawata, M. (1995) Roles of steroid hormones and their receptors in structural organization in the nervous system. *Neurosci. Res.* **24,** 1–46
2. Pfaff, D. W. (1997) Hormones, genes, and behavior. *Proc. Natl. Acad. Sci. U.S.A.* **94,** 14213–14216
3. Barbieri, R. L. (2008) Update in female reproduction: a life-cycle approach. *J. Clin. Endocrinol. Metab.* **93,** 2439–2446
4. Giguère, V., Yang, N., Segui, P., and Evans, R. M. (1988) Identification of a new class of steroid hormone receptors. *Nature* **331,** 91–94
5. Eudy, J. D., Yao, S., Weston, M. D., Ma-Edmonds, M., Talmadge, C. B., Cheng, J. J., Kimberling, W. J., and Sumegi, J. (1998) Isolation of a gene encoding a novel member of the nuclear receptor superfamily from the critical region of Usher syndrome type IIa at 1q41. *Genomics* **50,** 382–384
6. Kuiper, G. G., and Gustafsson, J. A. (1997) The novel estrogen receptor-β subtype: potential role in the cell- and promoter-specific actions of estrogens and anti-estrogens. *FEBS Lett.* **410,** 87–90
7. Giguère, V. (2008) Transcriptional control of energy homeostasis by the estrogen-related receptors. *Endocr. Rev.* **29,** 677–696
8. Hong, H., Yang, L., and Stallcup, M. R. (1999) Hormone-independent transcriptional activation and coactivator binding by novel orphan nuclear receptor ERR3. *J. Biol. Chem.* **274,** 22618–22626
9. Chen, S., Zhou, D., Yang, C., and Sherman, M. (2001) Molecular basis for the constitutive activity of estrogen-related receptor α-1. *J. Biol. Chem.* **276,** 28465–28470
10. Luo, J., Sladek, R., Carrier, J., Bader, J. A., Richard, D., and Giguère, V. (2003) Reduced fat mass in mice lacking orphan nuclear receptor estrogen-related receptor α. *Mol. Cell Biol.* **23,** 7947–7956
11. Huss, J. M., Imahashi, K., Dufour, C. R., Weinheimer, C. J., Courtois, M., Kovacs, A., Giguère, V., Murphy, E., and Kelly, D. P. (2007) The nuclear receptor ERRα is required for the bioenergetic and functional adaptation to cardiac pressure overload. *Cell Metab.* **6,** 25–37
12. LaBarge, S., McDonald, M., Smith-Powell, L., Auwerx, J., and Huss, J. M. (2014) Estrogen-related receptor-α (ERRα) deficiency in skeletal muscle impairs regeneration in response to injury. *FASEB J.* **28,** 1082–1097
13. Bookout, A. L., Jeong, Y., Downes, M., Yu, R. T., Evans, R. M., and Mangelsdorf, D. J. (2006) Anatomical profiling of nuclear receptor expression reveals a hierarchical transcriptional network. *Cell* **126,** 789–799
14. Alaynick, W. A., Kondo, R. P., Xie, W., He, W., Dufour, C. R., Downes, M., Jonker, J. W., Giles, W., Naviaux, R. K., Giguère, V., and Evans, R. M. (2007) ERRγ directs and maintains the transition to oxidative metabolism in the postnatal heart. *Cell Metab.* **6,** 13–24
15. Schreiber, S. N., Knutti, D., Brogli, K., Uhlmann, T., and Kralli, A. (2003) The transcriptional coactivator PGC-1 regulates the expression and activity of the orphan nuclear receptor estrogen-related receptor α (ERRα). *J. Biol. Chem.* **278,** 9013–9018
16. Dufour, C. R., Wilson, B. J., Huss, J. M., Kelly, D. P., Alaynick, W. A., Downes, M., Evans, R. M., Blanchette, M., and Giguère, V. (2007) Genome-wide orchestration of cardiac functions by the orphan nuclear receptors ERRα and -γ. *Cell Metab.* **5,** 345–356
17. Luo, J., Sladek, R., Bader, J. A., Matthyssen, A., Rossant, J., and Giguère, V. (1997) Placental abnormalities in mouse embryos lacking the orphan nuclear receptor ERR-β. *Nature* **388,** 778–782
18. Tremblay, G. B., Kunath, T., Bergeron, D., Lapointe, L., Champigny, C., Bader, J. A., Rossant, J., and Giguère, V. (2001) Diethylstilbestrol regulates trophoblast stem cell differentiation as a ligand of orphan nuclear receptor ERRβ. *Genes Dev.* **15,** 833–838
19. Bombail, V., MacPherson, S., Critchley, H. O., and Saunders, P. T. (2008) Estrogen receptor related β is expressed in human endometrium throughout the normal menstrual cycle. *Hum. Reprod.* **23,** 2782–2790
20. Watanabe, A., Kinoshita, Y., Hosokawa, K., Mori, T., Yamaguchi, T., and Honjo, H. (2006) Function of estrogen-related receptor α in human endometrial cancer. *J. Clin Endocrinol. Metab.* **91,** 1573–1577
21. Deblois, G., and Giguère, V. (2013) Oestrogen-related receptors in breast cancer: control of cellular metabolism and beyond. *Nat. Rev. Cancer* **13,** 27–36
22. Ijichi, N., Shigekawa, T., Ikeda, K., Horie-Inoue, K., Fujimura, T., Tsuda, H., Osaki, A., Saeki, T., and Inoue, S. (2011) Estrogen-related receptor γ modulates cell proliferation and estrogen signaling in breast cancer. *J. Steroid. Biochem. Mol. Biol.* **123,** 1–7
23. Lu, D., Kiriyama, Y., Lee, K. Y., and Giguère, V. (2001) Transcriptional regulation of the estrogen-inducible pS2 breast cancer marker gene by the ERR family of orphan nuclear receptors. *Cancer Res.* **61,** 6755–6761
24. Sun, P., Sehouli, J., Denkert, C., Mustea, A., Könsgen, D., Koch, I., Wei, L., and Lichtenegger, W. (2005) Expression of estrogen receptor-related receptors, a subfamily of orphan nuclear receptors, as new tumor biomarkers in ovarian cancer cells. *J. Mol. Med.* **83,** 457–467
25. Ariazi, E. A., Clark, G. M., and Mertz, J. E. (2002) Estrogen-related receptor α and estrogen-related receptor γ associate with unfavorable and favorable biomarkers, respectively, in human breast cancer. *Cancer Res.* **62,** 6510–6518
26. Suzuki, T., Miki, Y., Moriya, T., Shimada, N., Ishida, T., Hirakawa, H., Ohuchi, N., and Sasano, H. (2004) Estrogen-related receptor α in human breast carcinoma as a potent prognostic factor. *Cancer Res.* **64,** 4670–4676
27. Karimi, P., Hematti, S., Safari, F., and Tavassoli, M. (2013) Polymorphic AAAG repeat length in estrogen-related receptor γ (ERRγ) and risk of breast cancer in Iranian women. *Cancer Invest.* **31,** 600–603
28. Knower, K. C., Chand, A. L., Eriksson, N., Takagi, K., Miki, Y., Sasano, H., Visvader, J. E., Lindeman, G. J., Funder, J. W., Fuller, P. J., Simpson, E. R., Tilley, W. D., Leedman, P. J., Graham, J., Muscat, G. E., *et al.* (2013) Distinct nuclear receptor expression in stroma adjacent to breast tumors. *Breast Cancer Res. Treat.* **142,** 211–223
29. Lim, C. S., Baumann, C. T., Htun, H., Xian, W., Irie, M., Smith, C. L., and Hager, G. L. (1999) Differential localization and activity of the A- and B-forms of the human progesterone receptor using green fluorescent protein chimeras. *Mol. Endocrinol.* **13,** 366–375
30. Nishi, M., Takenaka, N., Morita, N., Ito, T., Ozawa, H., and Kawata, M. (1999) Real-time imaging of glucocorticoid receptor dynamics in living neurons and glial cells in comparison with non-neural cells. *Eur. J. Neurosci.* **11,** 1927–1936
31. Ochiai, I., Matsuda, K., Nishi, M., Ozawa, H., and Kawata, M. (2004) Imaging analysis of subcellular correlation of androgen receptor and estrogen receptor α in single living cells using green fluorescent protein color variants. *Mol. Endocrinol.* **18,** 26–42
32. Kaku, N., Matsuda, K., Tsujimura, A., and Kawata, M. (2008) Characterization of nuclear import of the domain-specific androgen receptor in association with the importin α/β and Ran-guanosine 5′-triphosphate systems. *Endocrinology* **149,** 3960–3969
33. Alexander, R. B., Greene, G. L., and Barrack, E. R. (1987) Estrogen receptors in the nuclear matrix: direct demonstration using monoclonal anti-receptor antibody. *Endocrinology* **120,** 1851–1857
34. Htun, H., Holth, L. T., Walker, D., Davie, J. R., and Hager, G. L. (1999) Direct visualization of the human estrogen receptor α reveals a role for ligand in the nuclear distribution of the receptor. *Mol. Biol. Cell* **10,** 471–486
35. Matsuda, K., Nishi, M., Takaya, H., Kaku, N., and Kawata, M. (2008) Intranuclear mobility of estrogen receptor α and progesterone receptors in association with nuclear matrix dynamics. *J. Cell. Biochem.* **103,** 136–148
36. Maruyama, K., Endoh, H., Sasaki-Iwaoka, H., Kanou, H., Shimaya, E., Hashimoto, S., Kato, S., and Kawashima, H. (1998) A novel isoform of rat estrogen receptor β with 18 amino acid insertion in the ligand binding domain as a putative dominant negative regular of estrogen action. *Biochem. Biophys. Res. Commun.* **246,** 142–147
37. Matsuda, K., Ochiai, I., Nishi, M., and Kawata, M. (2002) Colocalization and ligand-dependent discrete distribution of the estrogen receptor (ER) α and ERβ. *Mol. Endocrinol.* **16,** 2215–2230
38. Hashimoto, T., Matsuda, K., and Kawata, M. (2012) Scaffold attachment factor B (SAFB)1 and SAFB2 cooperatively inhibit the intranuclear mobility and function of ERα. *J. Cell. Biochem.* **113,** 3039–3050
39. Yoo, Y. A., Kim, Y. H., Kim, J. S., and Seo, J. H. (2008) The functional implications of Akt activity and TGF-β signaling in tamoxifen-resistant breast cancer. *Biochim. Biophys. Acta* **1783,** 438–447
40. Sekiguchi, M., Sudo, K., Suzuki, K., Matsuzawa, A., and Fujii, G. (1979) An ascites form of human mammary carcinoma transplantable in nude mice. *Biomedicine* **30,** 245–249

41. Nishi, M., Tanaka, M., Matsuda, K., Sunaguchi, M., and Kawata, M. (2004) Visualization of glucocorticoid receptor and mineralocorticoid receptor interactions in living cells with GFP-based fluorescence resonance energy transfer. *J. Neurosci.* **24,** 4918–4927
42. Stenoien, D. L., Patel, K., Mancini, M. G., Dutertre, M., Smith, C. L., O'Malley, B. W., and Mancini, M. A. (2001) FRAP reveals that mobility of oestrogen receptor-α is ligand- and proteasome-dependent. *Nat. Cell Biol.* **3,** 15–23
43. Mohseni, M., Cidado, J., Croessmann, S., Cravero, K., Cimino-Mathews, A., Wong, H. Y., Scharpf, R., Zabransky, D. J., Abukhdeir, A. M., Garay, J. P., Wang, G. M., Beaver, J. A., Cochran, R. L., Blair, B. G., Rosen, D. M., *et al.* (2014) MACROD2 overexpression mediates estrogen independent growth and tamoxifen resistance in breast cancers. *Proc. Natl. Acad. Sci. U.S.A.* **111,** 17606–17611
44. Lin, C. C., Tsai, Y. L., Huang, M. T., Lu, Y. P., Ho, C. T., Tseng, S. F., and Teng, S. C. (2006) Inhibition of estradiol-induced mammary proliferation by dibenzoylmethane through the E2-ER-ERE-dependent pathway. *Carcinogenesis* **27,** 131–136
45. Beato, M., Chávez, S., and Truss, M. (1996) Transcriptional regulation by steroid hormones. *Steroids* **61,** 240–251
46. Stenoien, D. L., Mancini, M. G., Patel, K., Allegretto, E. A., Smith, C. L., and Mancini, M. A. (2000) Subnuclear trafficking of estrogen receptor-α and steroid receptor coactivator-1. *Mol. Endocrinol.* **14,** 518–534
47. Barrack, E. R. (1987) Steroid hormone receptor localization in the nuclear matrix: interaction with acceptor sites. *J. Steroid Biochem.* **27,** 115–121
48. Shang, Y., Hu, X., DiRenzo, J., Lazar, M. A., and Brown, M. (2000) Cofactor dynamics and sufficiency in estrogen receptor-regulated transcription. *Cell* **103,** 843–852
49. Dong, S., Stenoien, D. L., Qiu, J., Mancini, M. A., and Tweardy, D. J. (2004) Reduced intranuclear mobility of APL fusion proteins accompanies their mislocalization and results in sequestration and decreased mobility of retinoid X receptor α. *Mol. Cell. Biol.* **24,** 4465–4475
50. Prüfer, K., Hernandez, C., and Gilbreath, M. (2008) Mutations in the AF-2 region abolish ligand-induced intranuclear immobilization of the liver X receptor α. *Exp. Cell Res.* **314,** 2652–2660
51. Brazda, P., Szekeres, T., Bravics, B., Tóth, K., Vámosi, G., and Nagy, L. (2011) Live-cell fluorescence correlation spectroscopy dissects the role of coregulator exchange and chromatin binding in retinoic acid receptor mobility. *J. Cell Sci.* **124,** 3631–3642
52. Muyan, M., Callahan, L. M., Huang, Y., and Lee, A. J. (2012) The ligand-mediated nuclear mobility and interaction with estrogen-responsive elements of estrogen receptors are subtype specific. *J. Mol. Endocrinol.* **49,** 249–266
53. Lavinsky, R. M., Jepsen, K., Heinzel, T., Torchia, J., Mullen, T. M., Schiff, R., Del-Rio, A. L., Ricote, M., Ngo, S., Gemsch, J., Hilsenbeck, S. G., Osborne, C. K., Glass, C. K., Rosenfeld, M. G., and Rose, D. W. (1998) Diverse signaling pathways modulate nuclear receptor recruitment of N-CoR and SMRT complexes. *Proc. Natl. Acad. Sci. U.S.A.* **95,** 2920–2925
54. Zhang, X., Jeyakumar, M., Petukhov, S., and Bagchi, M. K. (1998) A nuclear receptor corepressor modulates transcriptional activity of antagonist-occupied steroid hormone receptor. *Mol. Endocrinol.* **12,** 513–524
55. Zhou, W., Liu, Z., Wu, J., Liu, J. H., Hyder, S. M., Antoniou, E., and Lubahn, D. B. (2006) Identification and characterization of two novel splicing isoforms of human estrogen-related receptor β. *J. Clin. Endocrinol. Metab.* **91,** 569–579
56. Oftedal, B. E., Ladstein, S., Telle, W., and Male, R. (2005) Ligand-dependent protein interactions of the estrogen receptors using the yeast two-hybrid system. *Ann. N.Y. Acad. Sci.* **1040,** 420–425
57. Powell, E., and Xu, W. (2008) Intermolecular interactions identify ligand-selective activity of estrogen receptor α/β dimers. *Proc. Natl. Acad. Sci. U.S.A.* **105,** 19012–19017
58. Pettersson, K., Svensson, K., Mattsson, R., Carlsson, B., Ohlsson, R., and Berkenstam, A. (1996) Expression of a novel member of estrogen response element-binding nuclear receptors is restricted to the early stages of chorion formation during mouse embryogenesis. *Mech. Dev.* **54,** 211–223
59. Sem, D. S., Casimiro, D. R., Kliewer, S. A., Provencal, J., Evans, R. M., and Wright, P. E. (1997) NMR spectroscopic studies of the DNA-binding domain of the monomer-binding nuclear orphan receptor, human estrogen related receptor-2. The carboxyl-terminal extension to the zinc-finger region is unstructured in the free form of the protein. *J. Biol. Chem.* **272,** 18038–18043
60. Hentschke, M., Süsens, U., and Borgmeyer, U. (2002) Domains of ERRγ that mediate homodimerization and interaction with factors stimulating DNA binding. *Eur. J. Biochem.* **269,** 4086–4097
61. Sengupta, D., Bhargava, D. K., Dixit, A., Sahoo, B. S., Biswas, S., Biswas, G., and Mishra, S. K. (2014) ERRβ signalling through FST and BCAS2 inhibits cellular proliferation in breast cancer cells. *Br. J. Cancer* **110,** 2144–2158
62. Kumar, R., and Thompson, E. B. (2003) Transactivation functions of the N-terminal domains of nuclear hormone receptors: protein folding and coactivator interactions. *Mol. Endocrinol.* **17,** 1–10
63. Hall, J. M., and McDonnell, D. P. (2005) Coregulators in nuclear estrogen receptor action: from concept to therapeutic targeting. *Mol. Interv.* **5,** 343–357
64. Heery, D. M., Hoare, S., Hussain, S., Parker, M. G., and Sheppard, H. (2001) Core LXXLL motif sequences in CREB-binding protein, SRC1, and RIP140 define affinity and selectivity for steroid and retinoid receptors. *J. Biol. Chem.* **276,** 6695–6702
65. Kanaujiya, J. K., Lochab, S., Kapoor, I., Pal, P., Datta, D., Bhatt, M. L., Sanyal, S., Behre, G., and Trivedi, A. K. (2013) Proteomic identification of Profilin1 as a corepressor of estrogen receptor α in MCF7 breast cancer cells. *Proteomics* **13,** 2100–2112
66. Monroe, D. G., Secreto, F. J., Subramaniam, M., Getz, B. J., Khosla, S., and Spelsberg, T. C. (2005) Estrogen receptor α and β heterodimers exert unique effects on estrogen- and tamoxifen-dependent gene expression in human U2OS osteosarcoma cells. *Mol. Endocrinol.* **19,** 1555–1568
67. Horard, B., Castet, A., Bardet, P. L., Laudet, V., Cavailles, V., and Vanacker, J. M. (2004) Dimerization is required for transactivation by estrogen-receptor-related (ERR) orphan receptors: evidence from amphioxus ERR. *J. Mol. Endocrinol.* **33,** 493–509
68. Bombail, V., Collins, F., Brown, P., and Saunders, P. T. (2010) Modulation of ERα transcriptional activity by the orphan nuclear receptor ERRβ and evidence for differential effects of long- and short-form splice variants. *Mol. Cell. Endocrinol.* **314,** 53–61
69. Yu, S., Wong, Y. C., Wang, X. H., Ling, M. T., Ng, C. F., Chen, S., and Chan, F. L. (2008) Orphan nuclear receptor estrogen-related receptor-β suppresses *in vitro* and *in vivo* growth of prostate cancer cells via p21(WAF1/CIP1) induction and as a potential therapeutic target in prostate cancer. *Oncogene* **27,** 3313–3328
70. Heckler, M. M., and Riggins, R. B. (2015) ERRβ splice variants differentially regulate cell cycle progression. *Cell Cycle* **14,** 31–45